

# An Isolated Bidirectional Converter Modeling for Hybrid Electric Ship Simulations

Bijan Zahedi, Ole Christian Nebb, Lars Einar Norum

Norwegian University of Science and Technology

Electric Power Engineering Department

Emails: [bijan.zahedi@elkraft.ntnu.no](mailto:bijan.zahedi@elkraft.ntnu.no), [olechrne@stud.ntnu.no](mailto:olechrne@stud.ntnu.no), [norum@ntnu.no](mailto:norum@ntnu.no)

**Abstract-** Different modeling approaches for an isolated bidirectional dc-dc converter are investigated to be used in analysis and simulation of a hybrid electric ship. The models are verified by comparison with simulation results of detailed switching model in PLECS software. The advantages and disadvantages of different modeling methods are discussed. A unified model for both buck and boost modes is proposed for current control applications, using the preferable method. Finally, the simulation results of an energy storage system are presented, employing the proposed unified model in a hybrid electric ship simulation.

## INTRODUCTION

Bidirectional dc-dc converters are widely used in hybrid electric vehicles [1-5]. When used as energy storage interface, a bidirectional dc-dc converter operates in two modes of charge and discharge in order to absorb or deliver power. An isolated full-bridge dc-dc bidirectional converter is shown in Fig.1, which acts as a buck converter during charge period and as a boost converter during discharge. To study, design, and verify the system, different converter modeling methods are proposed in the literature [1-2, 6-7]. These will be discussed and compared in this paper.

A common approach for modeling the bidirectional converter reported in the literature is to use different models for each mode of operation [2]. From the system analysis point of view, in order to transfer from one mode to another in simulation, we need to switch between two models. Subsequently, two different controllers should be designed for two operating modes. The switching between models might also lead to certain error due to existing storage elements in the circuit (capacitors and inductors), unless residual charges from the previous operating mode are considered in the model. In addition, the transition between two modes leads to transient numerical errors and slow simulation. In case a unified model is developed, a single controller for both modes of operation would suffice. Besides, the problem of transferring between two modes in simulation would be resolved. A unified state space model for bidirectional converter is proposed in [1]. However, as it uses internal resistances of the sources, which are uncertain parameters, it cannot be appropriate in practice. This will be further discussed later in the paper.

In dc distribution of ships usually the task of voltage regulation is carried out by the primary energy source such as the generator-set. In such applications, in order to prevent

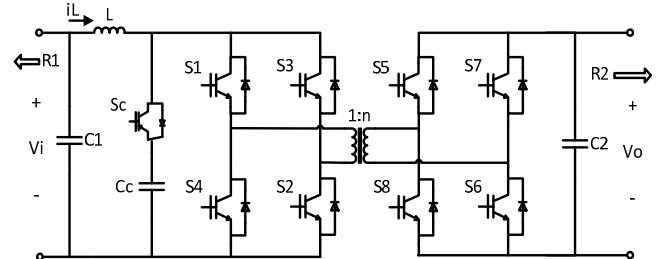


Fig. 1. The topological circuit of the bidirectional dc-dc converter under study

from conflicts in dc bus voltage control, the converter only takes care of its output current control while the bus voltage is applied as an input to the converter. Therefore, it is essential to adopt a converter model that is appropriate for current control.

In this paper, different modeling approaches are investigated for an isolated bidirectional dc-dc converter, to be used in the system analysis of hybrid electric ships. In order to verify different methods, all models are compared to the detailed switching model. The advantages and disadvantages of various methods including small signal averaging, nonlinear state space averaging, generalized averaging and the unified state space model [1] are discussed. Thereafter, this paper proposes a unified bidirectional converter model that suits current control applications. It will be shown that averaged switch modeling is the appropriate method to develop such a unified model. Finally, the simulation results of an energy storage system are presented, employing the proposed unified model in a hybrid electric ship simulation.

## MODELING OF THE CONVERTER IN TWO MODES

Power electronic devices have been already modeled by their detailed switching behavior in a number of standard software packages. However, the detailed switching models need extremely short time steps in simulation that leads to excessive simulation run time. As a solution, Average Value Modeling (AVM) is used, which makes the simulation orders of magnitude faster than that of the detailed model. Linearized AVM is used for small signal analysis through modeling the module by means of a few Transfer functions. Large signal analysis can be carried out by nonlinear AVM or nonlinear State Space AVM (SSAVM). In case ripple modeling is desired, the generalized averaging method can be

used [6]. Fig. 1 shows the bidirectional converter under study which has two modes of operation. Both modes will be modeled according to the mentioned methods.

#### A. Boost mode:

The differential equations of the boost mode are shown by (1)

$$\begin{cases} L \frac{di_L(t)}{dt} = v_{in}(t) - \frac{1}{n} (1 - u(t)) v_c(t) \\ C \frac{dv_c(t)}{dt} = \frac{1}{n} (1 - u(t)) i_L(t) - \frac{v_c(t)}{R} \end{cases} \quad (1)$$

where  $u(t) = \begin{cases} 1, & \text{for } 0 < t < dT \\ 0, & \text{for } dT < t < T \end{cases}$

The capacitor and resistor of the boost mode equations are  $C_2$  and  $R_2$  respectively, and the input voltage is  $V_1$  (Fig. 1).

#### I. Small signal model:

A fundamental approach to study the dynamic behavior of converters is to derive the small signal average model. It is performed by taking an average from the differential equations of (1) over switching period intervals

$$\begin{cases} L \frac{d\langle i_L(t) \rangle}{dt} = d(t) \langle v_{in}(t) \rangle + d'(t) \langle v_{in}(t) - \frac{1}{n} v_c(t) \rangle, \\ C \frac{d\langle v_c(t) \rangle}{dt} = d(t) \langle -\frac{v_c(t)}{R} \rangle + d'(t) \langle \frac{1}{n} i_L(t) - \frac{v_c(t)}{R} \rangle, \end{cases} \quad (2)$$

where  $\langle x(t) \rangle$  in equation (2) is the average of variable  $x$  over the switching period. Variable “d” is the duty cycle of the switching signal, and  $d' = 1 - d$ .

Based on (2), we obtain the small signal average model as (3), according to which we can develop a small signal ac equivalent circuit (Fig. 2).

$$\begin{cases} L \frac{d\hat{i}_L}{dt} = \hat{v}_{in} - \frac{D'}{n} \hat{v}_c + \frac{V_c}{n} \hat{d} \\ C \frac{d\hat{v}_c}{dt} = \frac{D'}{n} \hat{i}_L - \frac{1}{R} \hat{v}_c + \frac{I_L}{n} \hat{d} \end{cases} \quad (3)$$

where the capital letter notations are the design operating point values.

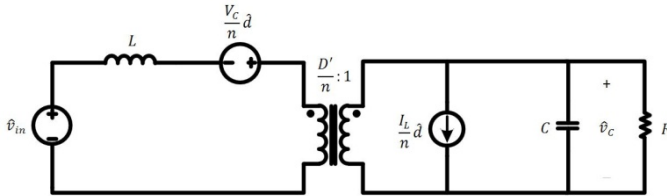


Fig. 2. Small signal ac equivalent circuit for the boost mode

The boost mode can also be shown in the block diagram form, which is suitable for linear control design. In this case, different transfer functions should be deduced from the small signal equivalent circuit. A complete block diagram for the

boost mode small signal model is shown in Fig. 3. The different transfer functions are expressed in the Appendix.

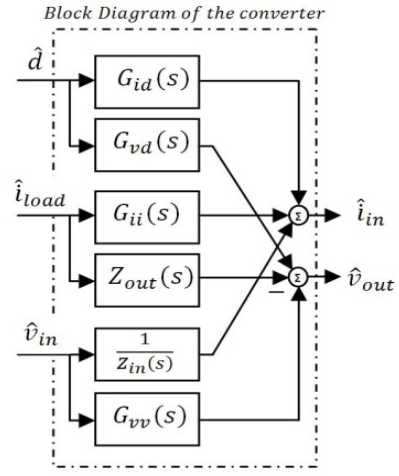


Fig. 3. Block diagram for the small signal model of the boost and buck modes based on transfer functions

#### 2. Large signal model:

The state space average model can also be expressed in a nonlinear form, to be appropriate for system level analysis. The state space equations are derived by expanding equation (1):

$$\begin{cases} \begin{bmatrix} \frac{di_L(t)}{dt} \\ \frac{dv_c(t)}{dt} \end{bmatrix} = \begin{bmatrix} 0 & -\frac{1}{nL} \\ \frac{1}{nC} & -\frac{1}{RC} \end{bmatrix} \begin{bmatrix} i_L(t) \\ v_c(t) \end{bmatrix} + \begin{bmatrix} \frac{1}{L} \\ 0 \end{bmatrix} v_{in}(t) & \text{for } 0 < t < dT, \\ \begin{bmatrix} \frac{di_L(t)}{dt} \\ \frac{dv_c(t)}{dt} \end{bmatrix} = \begin{bmatrix} 0 & 0 \\ 0 & -\frac{1}{RC} \end{bmatrix} \begin{bmatrix} i_L(t) \\ v_c(t) \end{bmatrix} + \begin{bmatrix} \frac{1}{L} \\ 0 \end{bmatrix} v_{in}(t) & \text{for } dT < t < T, \end{cases} \quad (4)$$

We can see that the boost mode is expressed by two sets of state space equations for two states of switching. By averaging over the switching period these two sets of equations will be combined in a single set of state space equation:

$$\begin{bmatrix} \frac{di_L(t)}{dt} \\ \frac{dv_c(t)}{dt} \end{bmatrix} = (d(t) \cdot \mathbf{A}_1 + (1 - d(t)) \cdot \mathbf{A}_2) \begin{bmatrix} i_L(t) \\ v_c(t) \end{bmatrix} + \mathbf{B} \cdot v_{in}(t) \quad (5)$$

where the matrices are as follows,

$$\mathbf{A}_1 \triangleq \begin{bmatrix} 0 & -\frac{1}{nL} \\ \frac{1}{nC} & -\frac{1}{RC} \end{bmatrix}, \quad \mathbf{A}_2 \triangleq \begin{bmatrix} 0 & 0 \\ 0 & -\frac{1}{RC} \end{bmatrix}, \quad \mathbf{B} \triangleq \begin{bmatrix} \frac{1}{L} \\ 0 \end{bmatrix}$$

Equation (5) represents the nonlinear state space average model of the boost mode. In order to model the ripples for higher accuracy, we can derive the generalized state-space

average model [6,8]. Then in the following section we will compare the different averaging methodologies.

### 3. Generalized average model:

In order to provide the generalized average model, we need to calculate the coefficients of Fourier series (6) for the circuit state variables based on (7). In this work, first harmonic approximation is performed ( $k = -1, 0, 1$ ).

$$x(t) = \sum_{k=-n}^n \langle x \rangle_k e^{jk\omega t}; \quad (6)$$

where  $\omega = 2\pi/T$

$$\langle x \rangle_k(t) = \frac{1}{T} \int_{t-T}^t x(\tau) e^{-jk\omega\tau} d\tau; \quad (7)$$

These Fourier coefficients are complex values, which are defined by (8) and (9). Taking the Fourier transform of (1) and replacing (8) and (9) into it, a new set of state-space equations are obtained whose state vector is  $[x_1 \ x_2 \ \dots \ x_6]^T$ . State space matrices A and B for the resulted state space model can be seen in [8].

$$\langle i_L \rangle_1 \triangleq x_1 + jx_2; \quad \langle i_L \rangle_0 \triangleq x_5; \quad \langle i_L \rangle_{-1} \triangleq \langle i_L \rangle_1^* \quad (8)$$

$$\langle v_C \rangle_1 \triangleq x_3 + jx_4; \quad \langle v_C \rangle_0 \triangleq x_6; \quad \langle v_C \rangle_{-1} \triangleq \langle v_C \rangle_1^* \quad (9)$$

$$i_L(t) = x_5 + 2x_1 \cos(\omega t) - 2x_2 \sin(\omega t); \quad (11)$$

$$v_C(t) = x_6 + 2x_3 \cos(\omega t) - 2x_4 \sin(\omega t); \quad (12)$$

Providing a time-invariant large signal state space model, software packages like Matlab/Simulink can be used to implement and control such a model.

### B. Buck mode:

The same procedure as for the boost mode modeling is performed for the buck mode. The final formulations of different methods for buck mode are expressed in the Appendix.

## SIMULATION OF THE CONVERTER IN TWO MODES

In order to investigate the explained modeling methods, the models are simulated, using Matlab®/Simulink®. The design parameters of the studied converter are given in Table I.

TABLE I  
DESIGN PARAMETERS OF THE CONVERTER UNDER STUDY

Parameters	Values	Parameters	Values
$V_{out}$	620 (V)	R	19.22 ( $\Omega$ )
$V_{in}$	100 (V)	C	267 $\mu F$
D	0.516	L	516 $\mu H$
$f_{sw}$	2 (kHz)	n	3

Fig. 4 illustrates the simulation results for average models of boost mode based on the open loop response to duty cycle step changes. It can be seen that the generalized SSAM

(GSSAM) shows the most accurate behavior which complies well with the detailed model. However, it is slow in simulation. Nonlinear SSAM is fast and accurate. It is suitable for system level studies, in which large signal analysis must be carried out. In case small signal analysis is desired, the linearized AVM is the best option; because the control design can be simply done by classical control theory.

Fig. 5 shows the open loop time response of the different buck models to duty cycle step changes. It can be seen that different models show satisfactory precision. The only difference is about the ripple (or pulsation) modeling. The generalized averaging by modeling the first order harmonic follows the ripples of the actual wave form; while the averaging methods are following only the dc value of the wave form. Since the input current in buck converters has an extremely pulsating waveform, the difference is particularly significant in current estimation. However, in case the purpose is to design the control system, the normal average models are preferred; because in control design the averaged values of variables matter.

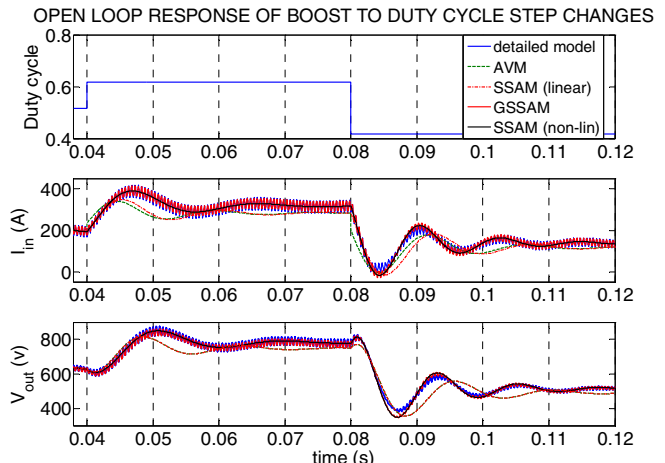


Fig. 4. Comparison of Open-loop duty cycle step response for boost mode

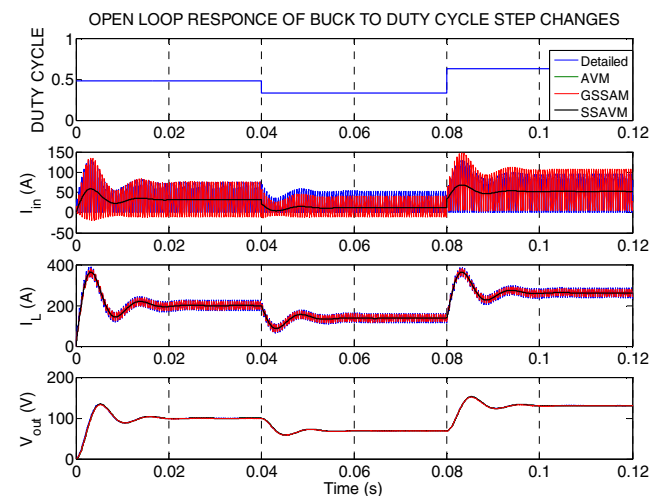


Fig. 5. Comparison of Open-loop duty cycle step response for buck mode

## UNIFIED MODEL FOR CURRENT CONTROL APPLICATIONS

### 1. Modeling suited to current control

The above-mentioned modeling methods can be appropriate when the dc voltage must be controlled. However, a problem shows up when it comes to those applications where current control is required. In such applications, the voltage must be applied to the converter as an input; whereas in small signal AVM and state space AVM, the voltage appears as an output or a state variable, respectively. In order to overcome this problem, the authors of [1-2] have introduced so-called “internal source resistances” through which the supply voltages are connected to the converter terminals. Involving these internal resistances into the circuit equations a “control to current transfer function” is obtained. However, it can be observed that the current control method proposed by these papers is to control the voltage drop across the internal source resistances whose values are extremely small and uncertain. Subsequently in practice a small change in the internal resistance leads to large error in the controlled current.

### 2. Merging into a unified model

In case we want to simulate a bidirectional converter, using the discussed methods, we can use two different models for two operating modes. Then, we have to switch between two mode models in order to transfer from one mode to another. The switching between models can lead to certain error due to existing storage elements in the circuit (capacitors and inductors), if their residual charges from the previous operating mode are not considered in the model. In addition, this transition between two modes not only leads to large transient errors in numerical analysis of the simulation program, it also moves the program away from convergence. This leads to extremely slow simulation when a mode transition occurs. Therefore, it seems necessary to develop a unified bidirectional converter model for system simulations. A unified model is also advantageous for controller design, as it requires only a single controller design for both modes of operation [1].

As a solution to the above challenges, we propose a unified model that suits current control applications, while being independent from uncertain parameters.

To achieve such a model, first, we have to express the output current in terms of converter variables rather than external imprecise parameters. It will be shown that it is possible by using the averaged switch modeling as follows. The first step is to simplify the switch network, which includes two H-bridges connected by a high frequency isolation transformer. Assuming ideal switches and transformer, the topology of Fig. 1 can be simplified to Fig. 6 for boost and buck modes of operation. The duty cycle of the new topology is the actual duty cycle divided by the transformer turn ratio.

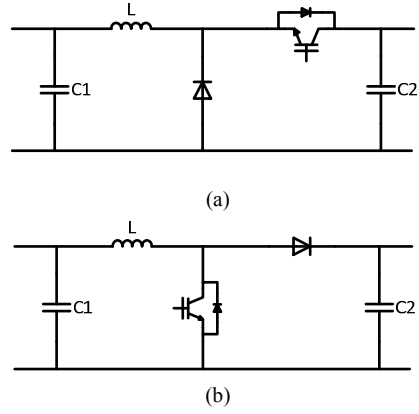


Fig. 6. Simplified topology of the bidirectional converter  
a) buck mode b) boost mode  
( $d_{\text{new}} = d_{\text{actual}}/n$ )

Using the averaged switch modeling [9], we obtain the averaged circuit for each mode as Fig. 7. In a bidirectional converter, the operation of the boost mode at duty cycle of “ $d'$ ” ( $=1-d$ ), corresponds to the operation of buck mode at duty cycle of “ $d$ ”, with only the opposite current direction. Therefore, the two models of Fig. 7 can be merged. The unified bidirectional converter model can be represented by Fig. 7.a.

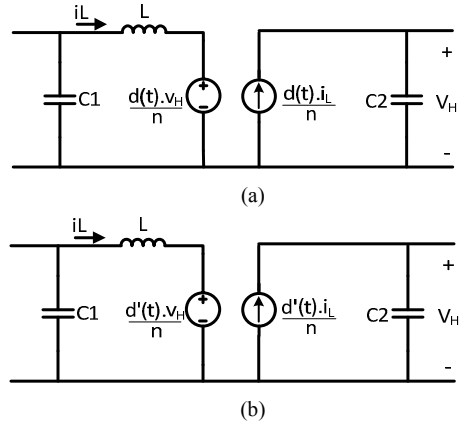


Fig. 7. Averaged switch model of the bidirectional converter  
a) buck mode b) boost mode  
(model.a can be used as a unified model since  $d'_{\text{discharge}} \equiv d_{\text{charge}}$ )

The simulation results of this unified model is illustrated in Fig. 8. This figure shows open-loop response to duty cycle step changes over a charge/discharge cycle. The low voltage side and high voltage side of the converter are supplied at their rated voltage levels. The figure shows that the proposed model complies with the detailed model. Such simulation cannot be carried out by the above-mentioned models, as they are not able to accept the voltages as inputs.

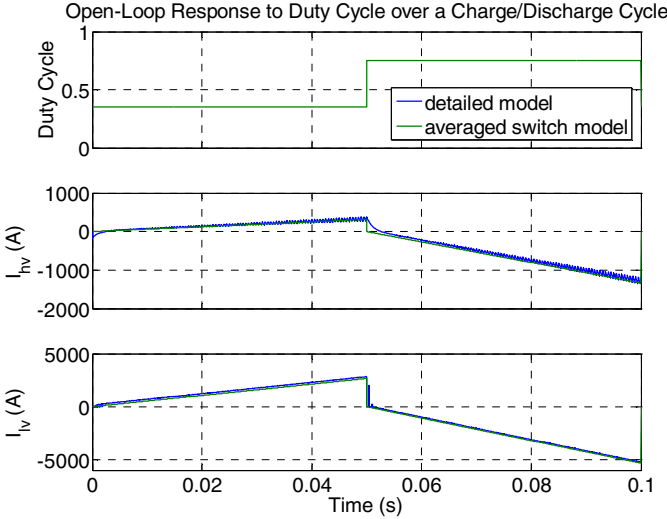


Fig. 8. Open loop response to duty cycle over a charge/discharge cycle

The proposed model is used in simulation of an energy storage system onboard a hybrid electric ship. The energy storage is a NiMH battery pack rated at 100V and 200Ah, which is connected to the ship dc distribution system through the bidirectional dc-dc converter. The dc bus voltage level is designed at 620V. Power share of the energy storage system is commanded and controlled through control of the dc current on high voltage side of the converter ( $I_{dc}$ ).

Fig. 9 shows a charge/discharge cycle of the battery when dc current is controlled on  $\pm 30A$ . It makes a comparison between the detailed model and averaged switch model by closed loop current control response to dc current step commands. The inversion-based control methodology [10] is used to control the converter model. The same control parameters are used to control the detailed switching model. The simulation results validate the proposed method, as acceptable agreement is found between the proposed model and the detailed model.

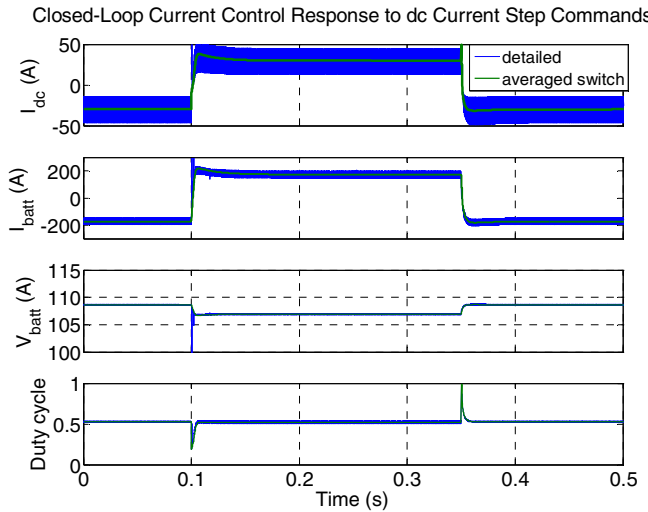


Fig. 9. Closed loop current control response to dc current step commands (charging/discharging the battery, the converter controls dc current on  $\pm 30A$ )

## CONCLUSION

Modeling of an isolated bidirectional dc-dc converter is discussed by comparison of a number of methods such as AVM, nonlinear SSAM, GSSAM, and averaged switch modeling. In order to verify different methods, all models have been compared to the detailed switching model. The application, advantages, and disadvantages of each modeling approach are addressed. The challenges of modeling the bidirectional converter for current control applications have been outlined. Then, an appropriate model to overcome the challenges is proposed. A straightforward unified bidirectional converter model suitable for current control applications is derived through averaged switch modeling method. The model has been validated against simulation results of the detailed switching model for both open loop response and closed loop current control.

## ACKNOWLEDGMENT

This research is supported by the Norwegian Research Council and Det Norske Veritas, under KMB project titled “Integrated Marine Electrical Power and Control Systems”.

## APPENDIX

### A) Buck Mode Formulation

#### 1. Small signal model:

The small signal model of the buck mode is expressed by the small signal differential equations.

$$\begin{cases} L \frac{d \hat{i}_L}{dt} = -\hat{v}_C + \frac{D}{n} \hat{v}_{in} + \frac{V_{in}}{n} \hat{d} \\ C \frac{d \hat{v}_C}{dt} = \hat{i}_L - \frac{1}{R} \hat{v}_C \\ \hat{i}_{in} = \frac{D}{n} \hat{i}_L + \frac{I_L}{n} \hat{d} \end{cases} \quad (\text{A.1})$$

#### 2. Large signal model:

Large signal model is expressed by the nonlinear form of state space averaging.

$$\left[ \begin{array}{l} \frac{di_L(t)}{dt} \\ \frac{dv_C(t)}{dt} \end{array} \right] = \mathbf{A} \begin{bmatrix} i_L(t) \\ v_C(t) \end{bmatrix} + (d(t) \cdot \mathbf{B}_1 + (1 - d(t)) \cdot \mathbf{B}_2) \cdot v_{in}(t) \quad (\text{A.2})$$

where the matrices are as follows,

$$\mathbf{A} \triangleq \begin{bmatrix} 0 & -\frac{1}{L} \\ \frac{1}{C} & -\frac{1}{RC} \end{bmatrix}, \quad \mathbf{B}_1 \triangleq \begin{bmatrix} \frac{1}{nL} \\ 0 \end{bmatrix}, \quad \mathbf{B}_2 \triangleq \begin{bmatrix} 0 \\ 0 \end{bmatrix}$$

### 3. Generalized averaging model:

The generalized average model is expressed by a state space equation whose state variables are defined as same as those of GASSM for boost mode.

$$\dot{\mathbf{X}} = \mathbf{AX} + \mathbf{BU} \quad (\text{A.3})$$

where the state matrices are as follows,

$$A = \begin{bmatrix} 0 & \omega & -1/L & 0 & 0 & 0 \\ -\omega & 0 & 0 & -1/L & 0 & 0 \\ 1/C & 0 & -1/RC & \omega & 0 & 0 \\ 0 & 1/C & -\omega & -1/RC & 0 & 0 \\ 0 & 0 & 0 & 0 & 0 & -1/L \\ 0 & 0 & 0 & 0 & 1/C & -1/RC \end{bmatrix}$$

$$B = \begin{bmatrix} D/nL & 0 & (\sin 2\pi d)/2n\pi L \\ 0 & D/nL & -(1-\cos 2\pi d)/2n\pi L \\ -(1-\cos \pi d)/2n\pi L & -(1-\cos \pi d)/2n\pi L & -(1-\cos \pi d)/2n\pi L \\ 0 & 0 & 0 \\ (\sin 2\pi d)/n\pi L & -(1-\cos 2\pi d)/n\pi L & D/nL \\ -(1-\cos \pi d)/2n\pi L & -(1-\cos \pi d)/2n\pi L & -(1-\cos \pi d)/2n\pi L \end{bmatrix}$$

### B) Transfer functions of Block Diagram "Fig.3"

TABLE A.1

	Buck	Boost
$G_{vv}(s)$	$\frac{D}{n} \frac{1}{1 + \frac{L}{R}s + LCS^2}$	$\frac{n}{D'} \frac{1}{1 + \frac{n^2L}{D'^2R}s + \frac{n^2LC}{D'^2}s^2}$
$G_{vd}(s)$	$\frac{V_{in}}{n} \frac{1}{1 + \frac{L}{R}s + LCS^2}$	$\frac{V_c}{D'} \frac{1 - \frac{n^2L}{D'^2R}s}{1 + \frac{n^2L}{D'^2R}s + \frac{n^2LC}{D'^2}s^2}$
$Z_{out}(s)$	$\frac{Ls}{1 + \frac{L}{R}s + LCS^2}$	$\frac{n^2L}{D'^2} \frac{s}{1 + \frac{n^2L}{D'^2R}s + \frac{n^2LC}{D'^2}s^2}$
$Z_{in}(s)$	$\frac{n^2R}{D^2} \frac{1 + \frac{L}{R}s + LCS^2}{RCs + 1}$	$\frac{D'^2R}{n^2} \frac{1 + \frac{n^2L}{D'^2R}s + \frac{n^2LC}{D'^2}s^2}{RCs + 1}$
$G_{id}(s)$	$\frac{DV_c}{n^2R} \left(1 + \frac{RCs + 1}{1 + \frac{L}{R}s + LCS^2}\right)$	$\frac{nV_c}{D'^2R} \left(1 + \frac{RCs + 1}{1 + \frac{n^2L}{D'^2R}s + \frac{n^2LC}{D'^2}s^2}\right)$
$G_{ii}(s)$	$\frac{D}{n} \frac{1}{1 + \frac{L}{R}s + LCS^2}$	$\frac{n}{D'} \frac{1}{1 + \frac{n^2L}{D'^2R}s + \frac{n^2LC}{D'^2}s^2}$

### REFERENCES

- [1] Junhong Zhang; Jih-Sheng Lai; Wensong Yu; "Bidirectional DC-DC converter modeling and unified controller with digital implementation," Applied Power Electronics Conference and Exposition, 2008. APEC 2008. Twenty-Third Annual IEEE, pp.1747-1753, 24-28 Feb. 2008
- [2] Il-Yop Chung, et al.; "Integration of a bi-directional dc-dc converter model into a large-scale system simulation of a shipboard MVDC power system", IEEE Electric Ship Technologies Symposium, pp. 318-325, April 2009
- [3] Urciuoli, D.P.; Tipton, C.W., "Development of a 90 kW bi-directional DC-DC converter for power dense applications," Applied Power Electronics Conference and Exposition, 2006. APEC '06. Twenty-First Annual IEEE, vol. no., pp.4 pp., 19-23 March 2006
- [4] J.-S. Lai, and D.J. Nelson, "Energy Management power converters in hybrid electric and fuel cell vehicles", in Proceedings of the IEEE, Vol. 95, No. 4, pp. 766 – 777, April 2007
- [5] M. Kabalo, B. Blunier, D. Bouquain and A. Miraoui, "State-of-the-art of DC-DC converters for fuel cell vehicles," in Vehicle Power and Propulsion Conference, Lile France, 2010
- [6] Emadi, A.; "Modeling and analysis of multiconverter DC power electronic systems using the generalized state-space averaging method," Industrial Electronics, IEEE Transactions on, vol.51, no.3, pp. 661-668, June 2004
- [7] Cho, H.Y.; Santi, E.; "Modeling and stability analysis in multi-converter systems including positive feedforward control", IEEE IECON Conference, pp. 839-844, Nov. 2008
- [8] Bijan Zahedi; Lars E. Norum; "Modeling, Analysis and Control of an Isolated Boost Converter for System Level Studies", Aegean Conference on Electric Machines and Power Electronics, Sept. 2011
- [9] Robert W. Erickson; "Fundamentals of Power Electronics", Kluwer Academic Publishers, 1999
- [10] P. J. Barré, A. Bouscayrol, P. Delarue, E. Dumetz, F. Giraud, J. P. Hautier, X. Kestelyn, B. Lemaire-Semail, and E. Semail, "Inversion-based control of electromechanical systems using causal graphical descriptions," in Proc. IEEE-IECON, Paris, France, pp. 5276–5281, Nov. 2006